Biochemical and Biophysical Research Communications 394 (2010) 909–914

Contents lists available at ScienceDirect

Biochemical and Biophysical Research Communications

journal homepage: www.elsevier.com/locate/ybbrc

Connexin 26 (GJB2) mutations, causing KID Syndrome, are associated with cell death due to calcium gating deregulation

Alessandro Terrinoni [a,*,1], Andrea Codispoti [a,1], Valeria Serra [a], Biagio Didona [b], Ernesto Bruno [c], Robert Nisticò [d,e], Michela Giustizieri [e], Marco Alessandrini [c], Elena Campione [f], Gerry Melino [a,g,**]

[a] Biochemistry Laboratory, IDI-IRCCS, C/O Department of Experimental Medicine and Biochemical Sciences, University of Rome "Tor Vergata", via Montpellier 1, 00133 Rome, Italy
[b] I Dermatological Division, IDI-IRCCS, via dei Monti di Creta, 104, Rome 00167, Italy
[c] ENT Department, University of Rome "Tor Vergata", 00133 Rome, Italy
[d] Department of Pharmacobiology, University of Calabria, via P. Bucci, Ed. Polifunzionale, 87036 Rende (CS), Italy
[e] Laboratory of Experimental Neurology, Fondazione Santa Lucia IRCCS, Rome, Italy
[f] Department of Diagnostic Imaging, University of Rome "Tor Vergata", Italy
[g] Medical Research Council, Toxicology Unit, Hodgkin Building, Leicester University, Lancaster Road, P.O. Box 138, Leicester LE1 9HN, UK

ARTICLE INFO

Article history:
Received 10 March 2010
Available online 15 March 2010

Keywords:
Connexin
Gap junctions
Mutations
KID Syndrome
Deafness
Cell death

ABSTRACT

The autosomic dominant KID Syndrome (MIM 148210), due to mutations in GJB2 (connexin 26, Cx26), is an ectodermal dysplasia with erythematous scaly skin lesions, keratitis and severe bilateral sensorineural deafness. The Cx26 protein is a component of gap junction channels in epithelia, including the cochlea, which coordinates the exchange of molecules and ions. Here, we demonstrate that different Cx26 mutants (Cx26D50N and Cx26G11E) cause cell death in vitro by the alteration of intra-cellular calcium concentrations. These results help to explain the pathogenesis of both the hearing and skin phenotypes, since calcium is also a potent regulator of the epidermal differentiation process.

1. Introduction

The autosomic dominant KID Syndrome (MIM 148210), caused by mutations in GJB2 (connexin 26, Cx26), [1] or GJB6 (connexin 30.3, Cx30.3) [2,3], is an ectodermal dysplasia which is normally included in the heterogeneous group of the erythrokeratodermias. At epidermal level, KID Syndrome shows localized erythematous scaly lesions and keratitis [4–14], with occasional scarring alopecia, while severe sensorineural deafness is evident at the hearing level. Further diagnostic features include corneal epithelial defects, scarring, and neo-vascularisation that could progress to blindness. Less than hundred cases have been reported so far [15–17].

Connexins share a common pattern of structural motifs, four trans-membrane (numbered from M1 to M4), two extra cellular, and three cytoplasmic domains: the amino-terminus, a cytoplasmic loop and the carboxy terminus domain. The two latter domains are characteristic of each connexin, while the membrane spanning and the extra cellular domains are highly conserved among the entire protein family [18–20]. The interaction of six connexins leads to the formation of a functional unit across the plasma membrane, called connexon or hemi-channel. Connexins can, therefore, interact in a homomeric or heteromeric way to form the connexon [19]. Connexons of adjacent cells form a channel (gap junction) [21] that is crucial for the rapid exchange of different molecules acting as secondary messengers or metabolites among two connected cells [18–20,22]. This seems particularly relevant for the recycling of potassium ions into the cochlear endolymph from the epithelial supporting cells to the spiral ligament and to the epithelial marginal cells of the stria vascularis [23,24]. The endocochlear potential in conjunction with the high K^+ of the endolymph are essential for the transduction of sound by the hair cells [25], and are therefore essential for normal hearing [23,26,27].

In this paper, we investigated the mechanism through which two Cx26 mutations identified in two clinical cases of KID

Abbreviations: Cx, connexin; PI, propidium iodide; FACS, fluorescence-activated cell sorter; GFP, green fluorescent protein; NHEK, normal human epidermal keratinocytes

* Corresponding author. Fax: +39 06 72596977.
** Corresponding author. Fax: +39 06 72596977.
E-mail addresses: alessandro.terrinoni@uniroma2.it (A. Terrinoni), gerry.melino@uniroma2.it, gm89@le.ac.uk (G. Melino).

[1] These two authors equally contributed to the work.

0006-291X/$ - see front matter Crown Copyright © 2010 Published by Elsevier Inc. All rights reserved.
doi:10.1016/j.bbrc.2010.03.073

Syndrome may result in the epidermal phenotype and sensorineural hearing loss.

2. Materials and methods

2.1. Cell culture transfection, Western blots and histology

Cryopreserved NHEK were obtained from BioWhittaker and grown in calf skin collagen-coated dishes in serum-free keratinocyte medium at 0.05 mM Ca^{2+}, supplemented with 7.5 μg/ml bovine pituitary extract, 0.5 mg/ml insulin, 0.5 mg/ml hydrocortisone, and 0.1 μg/ml hEGF. Third passage cells were used for experiments. Cells were treated for 1 and 3 days with 1.2 mM Ca^{2+}, 1 μM retinoic acid, and 250 ng/ml vitamin D3. SAOS2 cells were cultured in DMEM (Dulbecco's Modified Eagle Medium) adding FBS at 10%. Transfections have been realised using $CaPO^4$ (Invitrogen), Western blots have been realised according Candi et al. [28]. We used the following antibodies anti-GFP (Roche; diluizione 1/100), anti-actin (H-235, Santa Cruz, 1:1000); the signal has been revealed using ECL (Pierce).

Biopsy samples of the proband were taken and processed for light microscopy. Light microscopy samples were embedded in paraffin and stained with haematoxylin–eosin. Ethical approval and patient consent were obtained according guidelines of IDI-IRCCS Ethical Committee.

Fluorescence microscopy was performed on cells fixed with 4% paraformaldehyde, and then permeabilised with 0.25% Triton X-100 and stained 1 h with the appropriate antibody, following manufacturer instruction for concentration. Alexa fluor 488 (green) and 568 (red) antibodies where used as secondary antibodies. Nuclei were stained with DAPI 1 μg/ml.

2.2. Confocal microscopy

SAOS2 cells have been plated at density of 2.5–3 $\times$ 10^4 cells/cm^2 in chamber-slide and transfected using $CaPO^4$ (Invitrogen) according manufacturer instructions. Cells has been fixed using paraformaldehyde 4%, 10 min at RT, and permeabilised using PBS–Triton 0.25%. Cells has been stained using anti-Cx26 (Zymed lab; 1/100), anti-GFP (Roche; 1/100) and phalloidin-fitch (Sigma; 1/100). The fluorescence has been evaluated using Nikon, C1 on Eclipse TE200 and EZC1 software.

2.3. Cell cycle viability and apoptosis

Transfected cells have been harvested and centrifuged for 10 min at 1200 rpm, and after resuspended in ethanol 70%, at 4° for 2 h. RNase treatment has been performed for 15 min at 37 °C, using RNase in the final concentration of 20 μl/ml. Incubation with propidium iodide (50 μg/ml) for 20 min at 37 °C. Annexin V analysis has been performed harvesting both cells and supernatant. After centrifugation cells have been incubated in PBS (37 °C, 30 min), propidium iodide (2 μg/ml), and 5 μl of annexin V (Bender) in absence of light. Necrosis has been evaluated harvesting cells and supernatant and incubating them in PBS, 4 μg/ml of propidium iodide 100 nM di fluorescein di-acetate (FDA) for 5 min at RT, transferring samples on ice before cytofluorimetric analysis. Samples have been analysed using FACSCalibur (BD Biosciences, Mountain View, CA) and CellQuest software.

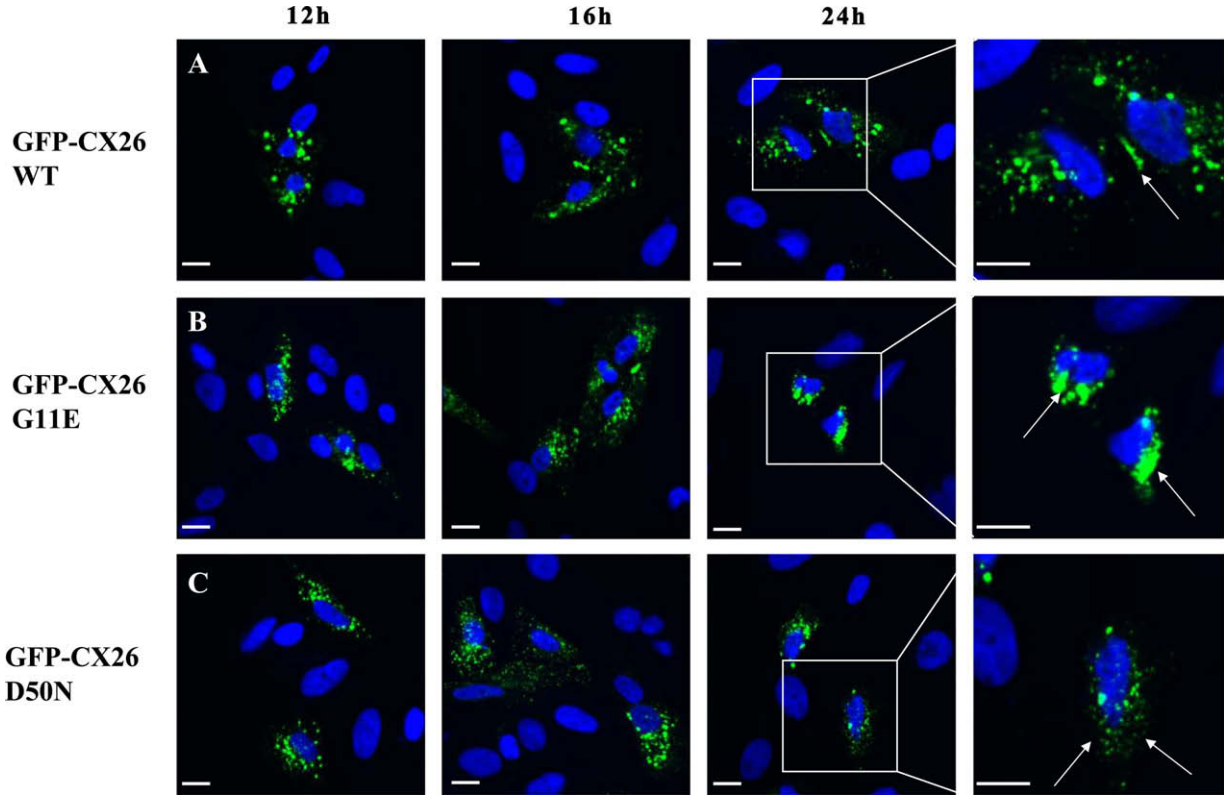

Fig. 1. Cellular distribution of wt and mutant connexin isoforms. Time course from 12 to 24 h of SAOS2 of transfection using WT (A), D50N (B) and G11E (C) GFP fusion constructs, nuclei have been stained using dapi (blue), GFP-cx26 is green. As is visible in the enlargement (A, last lane) WT connexin forms patches in plasma membrane and connexon structures in cells opposing surfaces (arrows). Otherwise the G11E fusion construct localizes in perinuclear collapsed cytoplasmic structures, characteristic of dying cells (B, last lane, arrows). (C) Mutant D50N also display problem of trafficking, but not perinuclear collapse (bar = 10 μm).

2.4. Cell internal calcium content and Imaging 5.13

Cultured cells have been harvested, and washed twice with PBS in absence of Ca^{2+} and Mg^{2+}, and than incubated with 5 μM di Fluo-3-AM (Invitrogen) for 30 min at 37 °C, in agitation, and in absence of light. Samples have been washed with HBSS with Ca^{2+} and Mg^{2+} and than analysed with FASCalibur (BD Biosciences, Mountain View, CA).

Internal concentration of calcium ions has been analysed using the Fura-2-AM (Molecular Probes) dye. Cells have been incubated in absence of light with 18 μl di Fura-2-AM in 1% FCS and 1% BSA, for 1 h at 37 °C. Cells have been subsequently washed 15% FCS medium and incubated for 1 h at 37 °C. Fluorescence has been evaluated using Axioscope FS (C. Zeiss).

3. Results

3.1. Protein trafficking and localization analysis

We identified two novel KID Syndrome patients with mutations in Cx at the residues G11E and D50N [29]. The mutated glycine 11 is localized in the cytoplasmic loop of the protein, involved in voltage and ion gating, while the other mutated residue (aspartic acid in position 50) is localized in the N-terminus adjacent to the M1 trans-membrane domain, also involved in voltage and ion gating, at the interaction between two opposing connexons [29]. We also reported that the expression of both mutant proteins is significantly reduced when compared to normal connexin 26. This suggests either a reduced protein stability of this mutant or that its over-expression results in cell death. To this aim, firstly we expressed the mutant proteins in vitro to evaluate their localization.

While the wild-type exogenous protein forms patches on the plasma membrane surface, characteristic of connexin proteins, as well as connexon structures in opposing surfaces (Fig. 1A, arrows in enlargement). When we over-expressed the G11E mutant in the small number of GFP-positive cells, the protein showed an altered cellular distribution. This mutant is localized in the cytoplasm around the nucleus, indicating an aggregation of cytoplasmic structures, while the nuclear condensation of these cells (Fig. 1B, arrows in enlargement) is suggestive of severe cell stress.

Also the over-expressed D50N construct shows an altered intracellular localization (Fig. 1C, arrows in enlargement), that clearly resembles problems of trafficking, typical of connexin mutations [30–36].

To further analyse the sub-cellular localization of the wt and mutated transgenes in a more physiological cellular model, we transfected normal human epithelial keratinocytes (NHEK) using expression vectors without GFP, and stained transfected cells with a specific Cx26 antibody. Again while the wt transgene, showed normal localization in the plasma membrane, with the characteristic patches of the hemi-channel arrays (Fig. 2A), the mutated proteins showed an increased intra-cellular localization, and a diffuse distribution pattern on the plasma membrane (Fig. 2B), demonstrating their inability to form structured hemi-channels. Specific confocal images of opposing cell surfaces, showed the presence of gap junction structures only in wt samples (Fig. 2, arrows in lane

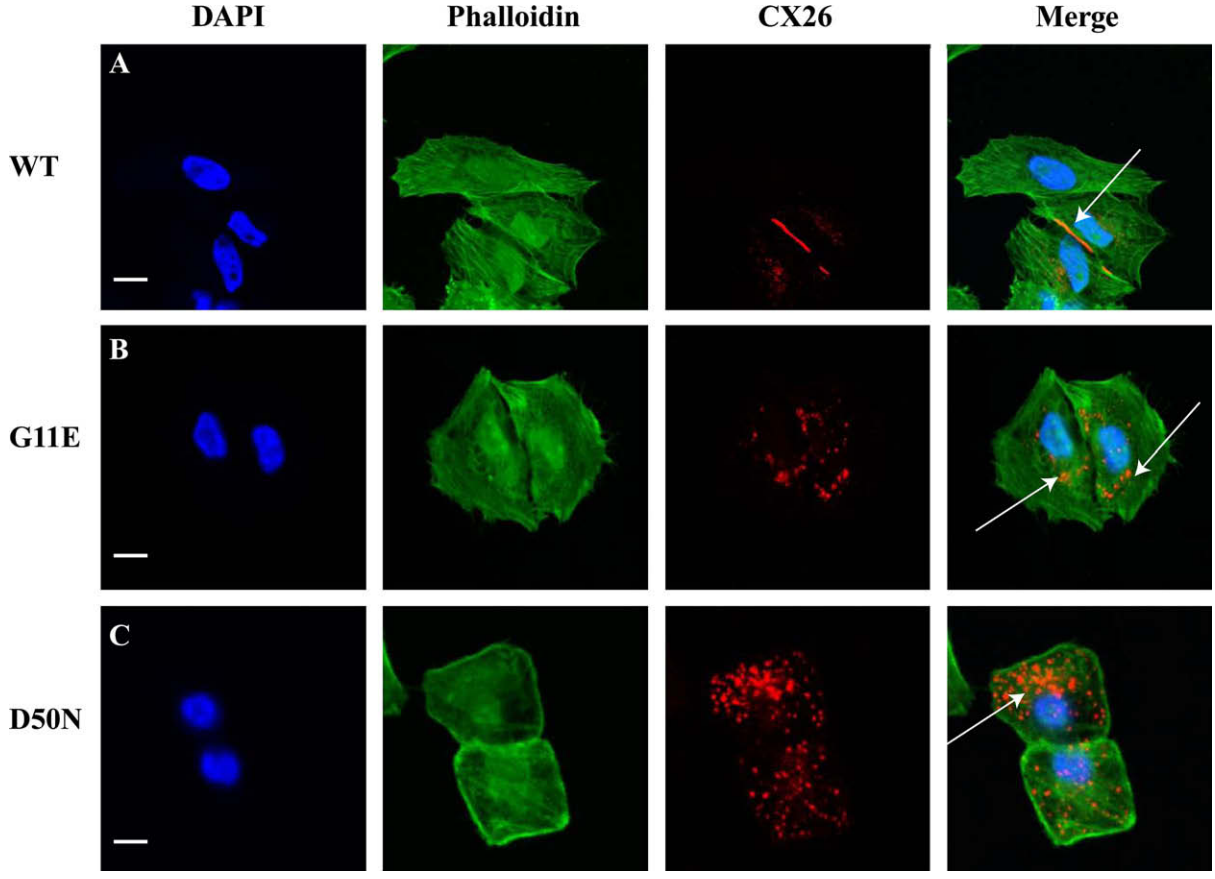

Fig. 2. Normal human epidermal keratinocyte analysis. (A) NHEK cells transfected with WT cx26 (anti-cx26 ab, red), dapi (blue) has been used for nuclei and phalloidin (green) has been used to visualize the cytoscheleton. The antibody stain connexon structures in opposing surfaces of contiguous cells. Patches on the membrane are also visible. (B) Transfection with G11E mutant reproduce perinuclear aggregates, while (C) using D50N mutant only problems of trafficking are revealed (bar = 20 μm).

A), while in the mutated G11E samples a perinuclear aggregation is seen (Fig. 2, arrows in lane B). In addition, the D50 N mutant also showed a cytoplasmic distribution without formation of hemichannels (Fig. 2, arrows in lane C). The same results were obtained in these cells using transgenes fused with GFP (data not shown).

3.2. Cell cycle and viability of cell transfected with wt and mutant connexines

To further investigate the biochemical and physiological role of the mutated connexins we investigated the effect on the cell cycle and cell death of cells transfected with wt and mutant connexins.

In keeping with the instability of the G11E mutant [29], positive cells were reduced after 24 h (Fig. 3A). Flow cytometry analysis of cells transfected with the different mutants and stained with annexin V and PI demonstrates that 53% of total cells transfected with this mutant are dead after 24 h, corresponding to almost 96% of Cx26 expressing cells. Conversely cells transfected with the wt only show 13% of dead cells (5% of Cx26 positive) while the D50N mutant shows an intermediate behaviour with approximately 23% of dead cells (8% of Cx26 positive). Our data also show that the majority of death occurs by necrosis rather than apoptosis (Fig. 3B–C) with PI positive and annexin negative cells. Indeed, fluorescein di-acetate (FDA) staining, confirms that death occurs largely by necrosis. Consistent with these results, all attempts to obtain clones stably expressing the G11E mutant failed.

To study the induced death in a "heterozygous state" we transfected wt/G11E mutant connexins at different ratios (Fig. 3D). The results show that increasing amounts of G11E result in increased death 24 h after the transfection; and at a 20/60 (wt/mut) ratio cell death is comparable to that obtained transfecting only the mutated form (Fig. 3D).

3.3. Ion gating of cells transfected with wt and mutant connexins

Gap junctions are physiologically important for the exchange of ions and small metabolites. Alterations of Na^+/K^+ levels and apoptosis have been previously shown in cells expressing the D50N mutation. Moreover, regulation of calcium ion fluxes is important in driving the epidermal differentiation of keratinocytes and its alteration can result in cell death by necrosis [37]. We therefore investigated free cytoplasmic calcium content, using Fluo-3AM in FACS analysis in cells transfected with our different constructs. Our results show that the free cytoplasmic calcium content is increased in samples with mutated connexines (Fig. 4A), and that higher levels of calcium are reached when transfecting the G11E mutant. Indeed, G11E transfection results in two fold more calcium than transfection of D50N, while this mutant only results in 0.4-fold increase of calcium as compared to the wt (Fig. 4A). Again decreasing the ratio wt/G11E mutant results in increased calcium levels, reaching a plateau at a 40/60 ratio (data not shown).

FACS analysis shows that cells transfected with the mutant G11E connexin increase their size, probably as a consequence of calcium uptake, starting from 12 h after transfection, and undergoing cell death between 12 and 24 h, as shown by the changes in light scattering (Fig. 4B–C).

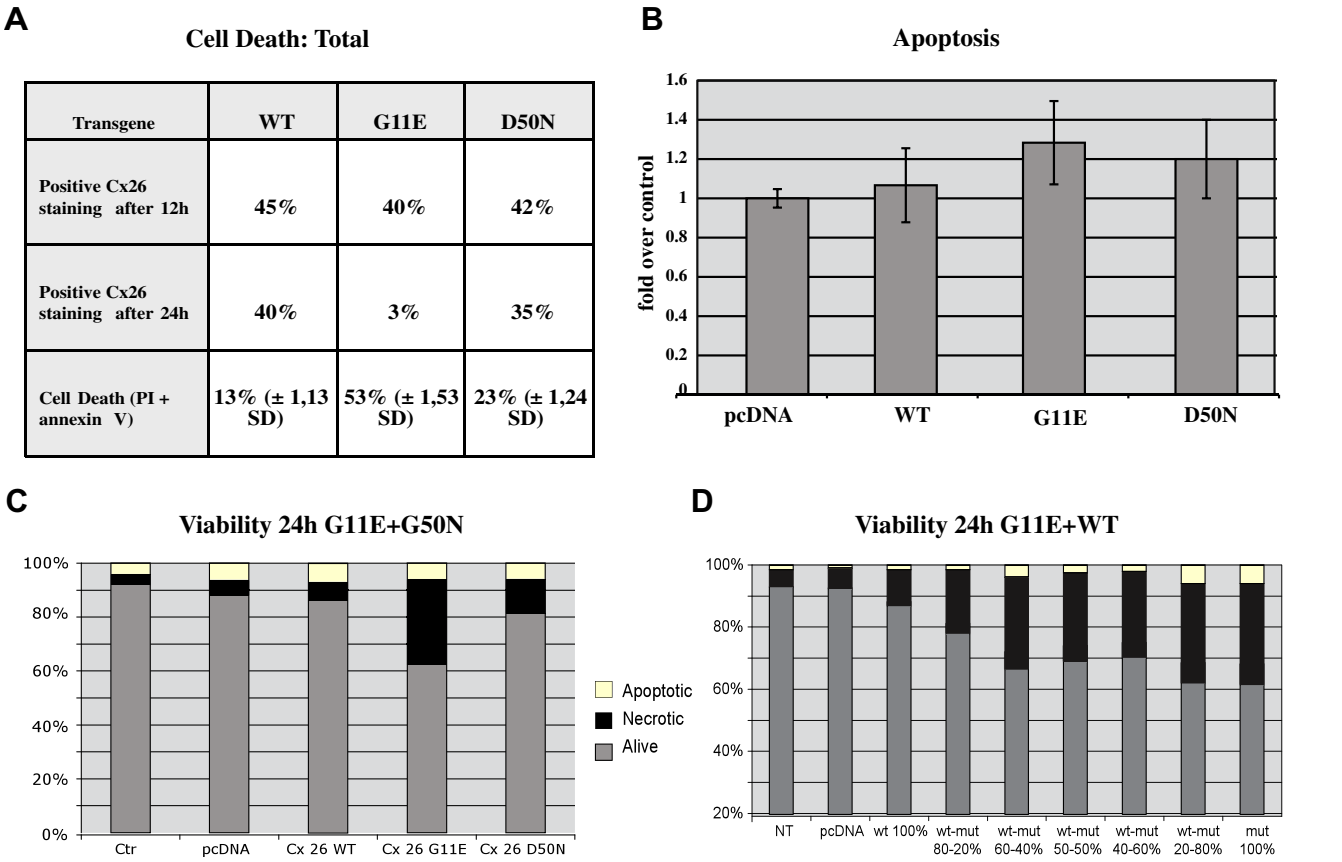

Fig. 3. Cell cycle and viability. (A) SAOS2 cells transfected with wt and mutant connexines. Positive cells counted using anti hcx26 antibody staining have been reported in graph, after 12 and 24 h of transfection. Total cell death have been analysed using propidium iodide and annexin V staining. (B) Apoptosis measured for each sample. (C) Viability analysis. In the graph are indicated the percent of apoptotic, necrotic and viable cells, evaluated by propidium iodide/fluorescein di-acetate double staining, demonstrating a strong effect of G11E on cell necrosis (red). (D) Viability of G11E transfected cells analysed using WT and mutated connexin to reproduce the heterozygous state. As it is visible in the graph, the G11E mutant strongly affects viability starting from a 60–40% WT/mut. (For interpretation of the references to color in this figure legend, the reader is referred to the web version of this paper.)

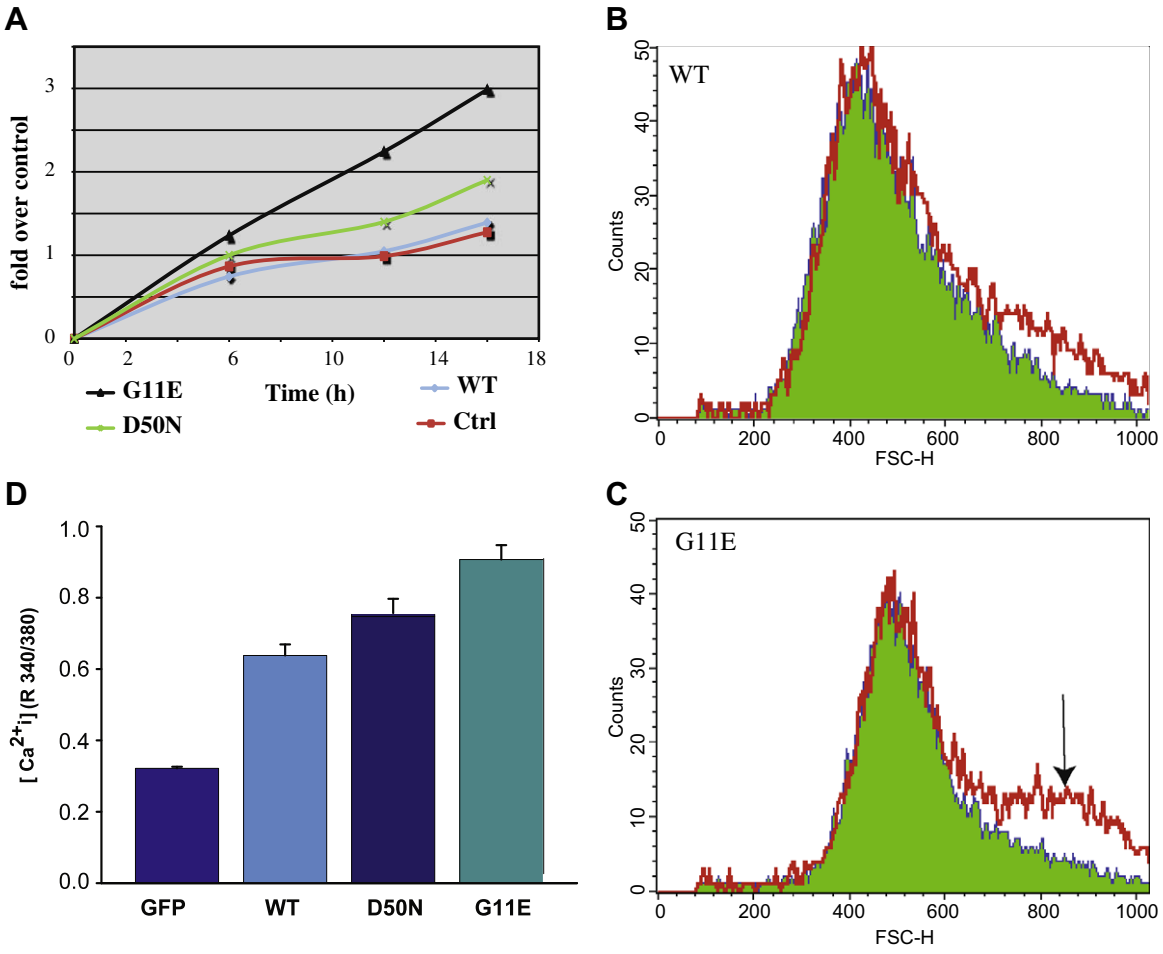

Fig. 4. Effect of connexin mutations on calcium levels. (A) The free cytoplasmic calcium content of control cells and cells transfected using WT and mutated connexines have been analysed with FACS analysis using Fluo-3-AM. The sample transfected with G11E construct reveal an internal global calcium concentration above two fold compared to the control, instead of the 0.4 of the D50N. (B and C) Forward scatter of cells analysed by FACS analysis showing that cells transfected with G11E mutant duplicate their size. (D) Calcium imaging performed using FURA-2 reagent demonstrates that generally the transfection with connexin increases basal calcium levels, but in cells expressing the G11E mutant the phenomenon becomes relevant.

To analyse only cells bearing mutant proteins we transfected NHEK cells with Cx26-GFP constructs, and to confirm this data we decided to perform electrophysiology experiments using FURA-2 for calcium imaging. Both fluorescence from GFP and from FURA-2 has been measured, and the level of the latter is shown in Fig. 4D. These results clearly indicate that single cells expressing both wt and mutated connexins increase their uptake of calcium (Fig. 4D).

Those observations indicate that a major function of Cx26 is the regulation of calcium flux, whose deregulation leads to predominantly necrotic death.

4. Discussion

Gap junction proteins are synthesized and co-translationally inserted in the endoplasmic reticulum membrane. After transport to the Golgi network they oligomerize to form hexameric hemi-channels called connexons, which are than transported to the plasma membrane and incorporated in gap junctional plaques [38]. Under physiological conditions the extra cellular portions of connexons interact with connexons of opposing cells in the intercellular space to complete functional active channels.

Even thought they are localized in different domains, G11E in the cytoplasmic loop, and D50N in the intra-cellular N-terminus adjacent to the M1 trans-membrane domain, both mutations analysed in this paper result in similar effects on cell physiology. However, while we can presume that the extracellular D50N mutation affects the interaction between connexons of adjacent cells, this is clearly not the case for the G11E mutation. G11E does show a predominant cytoplasmic perinuclear localization, as well as being less stable, and also does not form connexons (Figs. 1B and 2B). Thus, the end result of both mutations is an altered protein trafficking, resulting in abnormal connexon formation, due to a defect in the primary interaction and transportation within cell membranes after the production of the protein in the ER [33,34].

Recent data has correlated the D50N mutation with Na^+/K^+ channel deregulation and induction of apoptosis [39]. Our experiments demonstrate that, as well as resulting in apoptosis, expression of D50N also induces necrosis. Necrotic cell death is still more apparent when the G11E mutant is over-expressed, and still present at high levels G11E is expressed in equimolar concentrations with the wt allele. These data suggest that the deficiency in functional connexon formation by these mutant connexins results in aberrant calcium gating, leading to increased intra-cellular calcium and necrotic cell death. Indeed, the levels of both intra-cellular calcium and cell death are greater in the G11E than in the D50N-expressing cells.

Mutant connexins (V84L) deregulate the IP3 cascade, which is important in the Ca^{2+} pathway [40]. Our data show that the necrotic pathway is activated only when high levels of calcium are

reached, as with the G11E mutation and consequently, keratinocytes from the G11E patients failed to grow in culture. Consistent with our in vitro data, the patient with the D50N mutation has a milder clinical phenotype in both epidermis and hearing function. The massive necrosis of epidermal cells in the patient with the G11E mutation could lead to erythrodermia resulting in the marked hyperkeratosis observed in this patient. Similarly, the more pronounced destruction of Corti ciliate cells in the cochlea in the G11E patient would account for the more severe auditory deficit.

5. Conclusions

In brief, our data therefore provide a mechanistic explanation of the genotype–phenotype relationship, at least in these two mutations of KID Syndrome.

Acknowledgments

This work has been supported by the Medical Research Council, UK, "Alleanza contro il Cancro" (ACC), MIUR/PRIN (RBIP06L-CA9_0023), AIRC (2008-2010_33-08), ISS "Program Italia-USA" N526D5. Italian Human ProteomeNet RBRN07BMCT_007, Telethon (GGPO9133) and Ministero della Salute RF 06 73.2, RF07-57.

References

[1] G. Richard, F. Rouan, C.E. Willoughby, N. Brown, P. Chung, M. Ryynanen, E.W. Jabs, S.J. Bale, J.J. DiGiovanna, J. Uitto, L. Russell, Missense mutations in GJB2 encoding connexin-26 cause the ectodermal dysplasia keratitis–ichthyosis–deafness syndrome, Am. J. Hum. Genet. 70 (2002) 1341–1348.
[2] F. Macari, M. Landau, P. Cousin, B. Mevorah, S. Brenner, R. Panizzon, D.F. Schorderet, D. Hohl, M. Huber, Mutation in the gene for connexin 30.3 in a family with erythrokeratodermia variabilis, Am. J. Hum. Genet. 67 (2000) 1296–1301.
[3] A.Y. Jan, S. Amin, P. Ratajczak, G. Richard, V.P. Sybert, Genetic heterogeneity of KID syndrome: identification of a Cx30 gene (GJB6) mutation in a patient with KID syndrome and congenital atrichia, J. Invest. Dermatol. 122 (2004) 1108–1113.
[4] N. Alli, E. Gungor, Keratitis, ichthyosis and deafness (KID) syndrome, Int. J. Dermatol. 36 (1997) 37–40.
[5] H. Caceres-Rios, L. Tamayo-Sanchez, C. Duran-Mckinster, M. de la Luz Orozco, R. Ruiz-Maldonado, Keratitis, ichthyosis, and deafness (KID syndrome): review of the literature and proposal of a new terminology, Pediatr. Dermatol. 13 (1996) 105–113.
[6] D.L. Cram, J.S. Resneck, W.B. Jackson, A congenital ichthyosiform syndrome with deafness and keratitis, Arch. Dermatol. 115 (1979) 467–471.
[7] I. Kone-Paut, S. Hesse, C. Palix, R. Rey, K. Remediani, J.M. Garnier, P. Berbis, Keratitis, ichthyosis, and deafness (KID) syndrome in half sibs, Pediatr. Dermatol. 15 (1998) 219–221.
[8] K. Langer, K. Konrad, K. Wolff, Keratitis, ichthyosis and deafness (KID)-syndrome: report of three cases and a review of the literature, Br. J. Dermatol. 122 (1990) 689–697.
[9] J.D. McGrae Jr., Keratitis, ichthyosis, and deafness (KID) syndrome, Int. J. Dermatol. 29 (1990) 89–93.
[10] M.R. Morris, A. Namon, G.Y. Shaw, W.R. Panje, E.E. Mhoon, The keratitis, ichthyosis, and deafness syndrome, Otolaryngol. Head Neck Surg. 104 (1991) 526–528.
[11] D.S. Nurse, Keratitis, ichthyosis, deafness (KID) syndrome, Clin. Exp. Dermatol. 19 (1994) 280.
[12] R.J. Rycroft, E.J. Moynahan, R.S. Wells, Atypical ichthyosiform erythroderma deafness and keratitis. A report of two cases, Br. J. Dermatol. 94 (1976) 211–217.
[13] K. Singh, Keratitis, ichthyosis and deafness (KID syndrome), Australas J. Dermatol. 28 (1987) 38–41.
[14] B.A. Skinner, M.C. Greist, A.L. Norins, The keratitis, ichthyosis, and deafness (KID) syndrome, Arch. Dermatol. 117 (1981) 285–289.
[15] G. Richard, N. Brown, L.E. Smith, A. Terrinoni, G. Melino, R.M. Mackie, S.J. Bale, J. Uitto, The spectrum of mutations in erythrokeratodermias – novel and de novo mutations in GJB3, Hum. Genet. 106 (2000) 321–329.
[16] J. Mazereeuw-Hautier, E. Bitoun, J. Chevrant-Breton, S.Y. Man, C. Bodemer, C. Prins, C. Antille, J.H. Saurat, D. Atherton, J.I. Harper, D.P. Kelsell, A. Hovnanian, Keratitis–ichthyosis–deafness syndrome: disease expression and spectrum of connexin 26 (GJB2) mutations in 14 patients, Br. J. Dermatol. 156 (2007) 1015–1019.
[17] M.A. van Steensel, Gap junction diseases of the skin, Am. J. Med. Genet. C Semin. Med. Genet. 131C (2004) 12–19.
[18] D.A. Goodenough, J.A. Goliger, D.L. Paul, Connexins, connexons, and intercellular communication, Annu. Rev. Biochem. 65 (1996) 475–502.
[19] N.M. Kumar, N.B. Gilula, The gap junction communication channel, Cell 84 (1996) 381–388.
[20] G. Mese, G. Richard, T.W. White, Gap junctions: basic structure and function, J. Invest. Dermatol. 127 (2007) 2516–2524.
[21] M. Yeager, B.J. Nicholson, Structure of gap junction intercellular channels, Curr. Opin. Struct. Biol. 6 (1996) 183–192.
[22] R. Bruzzone, T.W. White, D.L. Paul, Connections with connexins: the molecular basis of direct intercellular signaling, Eur. J. Biochem. 238 (1996) 1–27.
[23] J.R. Holt, D.P. Corey, Ion channel defects in hereditary hearing loss, Neuron 22 (1999) 217–219.
[24] K.P. Steel, One connexin, two diseases, Nat. Genet. 20 (1998) 319–320.
[25] M.G. Evans, C.J. Kros, The cochlea – new insights into the conversion of sound into electrical signals, J. Physiol. 576 (2006) 3–5.
[26] A. Terrinoni, G. Melino, V. Serra, M. Alessandrini, B. Napolitano, E. Bruno, Deafness, in: Encyclopedia of Life Sciences (ELS), John Wiley & Sons Ltd., Chichester, 2009.
[27] R. Rabionet, L. Zelante, N. Lopez-Bigas, L. D'Agruma, S. Melchionda, G. Restagno, M.L. Arbones, P. Gasparini, X. Estivill, Molecular basis of childhood deafness resulting from mutations in the GJB2 (connexin 26) gene, Hum. Genet. 106 (2000) 40–44.
[28] E. Candi, A. Rufini, A. Terrinoni, D. Dinsdale, M. Ranalli, A. Paradisi, V. De Laurenzi, L.G. Spagnoli, M.V. Catani, S. Ramadan, R.A. Knight, G. Melino, Differential roles of p63 isoforms in epidermal development: selective genetic complementation in p63 null mice, Cell Death Differ. 13 (2006) 1037–1047.
[29] A. Terrinoni, A. Codispoti, V. Serra, E. Bruno, B. Didona, M. Paradisi, R. Nisticò, E. Campione, L. Diluvio, G. Melino, Connexin 26 (GJB2) mutations as a cause of the KID Syndrome with hearing loss, Biochem. Biophys. Res. Commun. (2010). doi:10.1016/j.bbrc.2010.03.098.
[30] J.W. Kyle, P.J. Minogue, B.C. Thomas, D.A. Domowicz, V.M. Berthoud, D.A. Hanck, E.C. Beyer, An intact connexin N-terminus is required for function but not gap junction formation, J. Cell Sci. 121 (2008) 2744–2750.
[31] T.D. Matos, H. Caria, H. Simoes-Teixeira, T. Aasen, O. Dias, M. Andrea, D.P. Kelsell, G. Fialho, A novel M163L mutation in connexin 26 causing cell death and associated with autosomal dominant hearing loss, Hear. Res. 240 (2008) 87–92.
[32] E.A. de Zwart-Storm, H. Hamm, J. Stoevesandt, P.M. Steijlen, P.E. Martin, M. van Geel, M.A. van Steensel, A novel missense mutation in GJB2 disturbs gap junction protein transport and causes focal palmoplantar keratoderma with deafness, J. Med. Genet. 45 (2008) 161–166.
[33] E. Thonnissen, R. Rabionet, M.L. Arbones, X. Estivill, K. Willecke, T. Ott, Human connexin26 (GJB2) deafness mutations affect the function of gap junction channels at different levels of protein expression, Hum. Genet. 111 (2002) 190–197.
[34] W.L. Di, J. Monypenny, J.E. Common, C.T. Kennedy, K.A. Holland, I.M. Leigh, E.L. Rugg, D. Zicha, D.P. Kelsell, Defective trafficking and cell death is characteristic of skin disease-associated connexin 31 mutations, Hum. Mol. Genet. 11 (2002) 2005–2014.
[35] A. Terrinoni, A. Leta, C. Pedicelli, E. Candi, M. Ranalli, P. Puddu, M. Paradis, C. Angelo, G. Bagetta, G. Melino, A novel recessive connexin 31 (GJB3) mutation in a case of erythrokeratodermia variabilis, J. Invest. Dermatol. 122 (2004) 837–839.
[36] A. Terrinoni, G. Melino, Recessive EKV, J. Invest. Dermatol. 124 (2004) 270–271.
[37] W.X. Zong, C.B. Thompson, Necrotic death as a cell fate, Genes Dev. 20 (2006) 1–15.
[38] D.W. Laird, Life cycle of connexins in health and disease, Biochem. J. 394 (2006) 527–543.
[39] J.R. Lee, A.M. Derosa, T.W. White, Connexin mutations causing skin disease and deafness increase hemi-channel activity and cell death when expressed in Xenopus oocytes, J. Invest. Dermatol. 129 (2009) 870–878.
[40] M. Beltramello, V. Piazza, F.F. Bukauskas, T. Pozzan, F. Mammano, Impaired permeability to Ins(1,4,5)P3 in a mutant connexin underlies recessive hereditary deafness, Nat. Cell Biol. 7 (2005) 63–69.